Physica E 130 (2021) 114712

Contents lists available at ScienceDirect

Physica E: Low-dimensional Systems and Nanostructures

journal homepage: http://www.elsevier.com/locate/physe

Radius dependence of the electrical conductivity of zigzag carbon nanotubes

M. Amekpewu, Ph.D, Senior Lecturer [a,*], S.Y. Mensah, Ph.D, Professor [b], R. Musah, Ph. D, Senior Lecturer [a], S.S. Abukari, Ph.D, Associate Professor [b], N.G. Mensah, Ph.D, Associate Professor [c], K. A. Dompreh, Ph. D, Senior Lecturer [b]

[a] Department of Applied Physics, C. K. Tedam University of Technology and Applied Sciences, Navrongo, Ghana
[b] Department of Physics, College of Agriculture and Natural Sciences, U.C.C, Ghana
[c] Department of Mathematics, College of Agriculture and Natural Sciences, U.C.C, Ghana

ARTICLE INFO

Keywords:
Carbon nanotube
Conductivity
Radius
Current density
dc field

ABSTRACT

The radius dependence of the electrical conductivity of metallic and semiconducting zigzag carbon nanotubes (CNTs) is theoretically studied. The investigation was done semiclassically by solving the Boltzmann transport equation to derive current density as a function of a homogenous axial dc field and radius of the tube. The analysis was numerically carried out by varying the radius of the materials at a constant temperature. Plots of the normalized current density versus dc field applied along the axis of both materials are presented. We observed that in the case of the metallic zigzag CNTs as the radius increases, the electrical conductivity decreases. On the other hand, in the semiconducting zigzag CNT there was an increase as radius increases. This research shows that thinner metallic zigzag CNTs and thicker semiconducting zigzag CNTs are better conductors of electricity. This investigation therefore offers way of obtaining higher electrical conductivity in both materials without doping. This study therefore shows applications in the development of current conducting nano-devices for scientific systems.

1. Introduction

The structure of carbon nanotube (CNT) consists of enrolled cylindrical graphitic sheet (called graphene) rolled up into a seamless cylinder with diameter of the order of a nanometre [1]. Depending on the arrangement of carbon atoms in a given CNT or how the two-dimensional graphite sheet is rolled up, they can be classified as chiral (n, m) CNT, armchair (n, n) CNT, $n = m$ and zigzag (n, 0) CNT, $m = 0$ [2,3]. The integers n and m are called chiral indices of CNT which denote the numbers of unit vectors along two directions in the hexagonal lattice of graphite sheet (or graphene) rolled up seamlessly to form the CNT [1–4]. For a given (n, m) CNT, if $2n + m = 3i$ or n-$m = 3i$, (where i is an integer and $n \geq m$), then the CNT is a metal, otherwise the CNT is a semiconductor [5]. This leads to the cases that all armchairs (n, n) CNTs are metallic or conducting, and zigzag (n, 0) CNTs are only metallic or conducting if n is a multiple of 3. The thinness of any type of CNT which is a function of the radius of CNT depends on the integers n and m [6]. It has been reported that CNTs conduct electricity better than copper [7]. Due to the impressive list of attributes of CNTs [8], they have a wide variety of possible applications [9–15].

There are various reports on Negative Differential Conductivity (NDC) in CNTs [16–19]. However, to the best of our knowledge, a report on impact of the radius of zigzag (n, 0) CNT on its electrical conductivity is limited. Thus, in this paper, we present theoretical framework investigations of radius dependence of the electrical conductivity of either metallic or semiconducting zigzag (n, 0) CNT using the semiclassical Boltzmann's transport equation to derive current density along the tube's axis.

2. Theory

The effect of space charge inside CNT was neglected since space charge injection and accumulation are suppressed to a large extent under 400 kV/cm [20] and so relatively low maximum dc field of 150

* Corresponding author.
E-mail addresses: mamekpewu@cktutas.edu.gh (M. Amekpewu), profsymensah@gmail.com (S.Y. Mensah), rmusah@cktutas.edu.gh (R. Musah), sulemana70@gmail.com (S.S. Abukari), nmensah3@ucc.edu.gh (N.G. Mensah), kwadwo.dompreh@ucc.edu.gh (K.A. Dompreh).

https://doi.org/10.1016/j.physe.2021.114712
Received 7 December 2020; Received in revised form 19 February 2021; Accepted 26 February 2021
Available online 1 March 2021

kV/cm was used throughout the study. If a homogenous dc field E_{ax} is applied along the axis of an undoped single-walled zigzag (n, 0) CNT, the electrons obey semiclassical Newton's law when scattering is neglected [21], we obtained

$$\frac{dP_{ax}}{dt} = eE_{ax} \tag{1}$$

where P_{ax} , t and e are the axial component of the quasimomentum, time taken and the electronic charge of the propagating electrons respectively. For a CNT, the energy level spacing $\Delta\varepsilon$ is given by Ref. [16],

$$\Delta\varepsilon = \pi\hbar V_F/L \tag{2}$$

where $\hbar = h/2\pi$, h is Planck constant, V_F is Fermi velocity and L is the length of the nanotube. The investigation is done within the semiclassical approximation in which the motion of the π-electrons is considered as classical motion of free quasiparticles in the field of the crystalline lattice with dispersion law extracted from the quantum theory [16]. Taking into account the hexagonal crystalline structure of a rolled graphene in a form of CNT and using the tight binding approximation, the energy for zigzag (n, 0)CNT is expressed as in equation (3) [22],

$$\begin{aligned}\varepsilon(s\Delta p_\varphi, p_{ax}) &\equiv \varepsilon_s(p_{ax}) \\ &= \pm\gamma_0\left[1 + 4cos(ap_{ax})cos\left(\frac{a}{\sqrt{3}}s\Delta p_\varphi\right) + 4cos^2\left(\frac{a}{\sqrt{3}}s\Delta p_\varphi\right)\right]^{1/2}\end{aligned} \tag{3}$$

where a is the lattice constant of the zigzag (n, 0) CNT, $\gamma_0 \approx 3.0$eV is the overlapping integral, p_{ax} is the axial component of quasimomemtum. Δp_φ is transverse quasimomentum level spacing and s is an integer. The expression for lattice constant a in equation (3) is given by

$$a = \frac{3a_{c-c}}{2\hbar} \tag{4}$$

where $a_{c-c} = 0.142$ nm is the C–C bond length.

The - and + signs correspond to the valence and conduction bands respectively. Due to the transverse quantization of the quasimomentum P, its transverse component p_φ can take n discrete values [16],

$$p_\varphi = s\Delta p_\varphi = s\frac{\pi\sqrt{3}}{an}, \quad (s = 1, \ldots, n) \tag{5}$$

Unlike transverse quasimomentum, p_φ, the axial quasimomentum p_{ax} is assumed to vary continuously within the range $0 \le p_{ax} \le 2\pi/a$, which corresponds to the model of infinitely long CNT ($L = \infty$). This model is applicable to the case under consideration because we are restricted to temperatures and/or voltages well above the level spacing [16], i.e. $k_BT > \varepsilon_c, \Delta\varepsilon$, where k_B is Boltzmann constant, T is the temperature; ε_c is the charging energy. Considering the motion of quasiparticles in an external axial electric field which is described by the Boltzmann kinetic equation is given by [16,21]

$$\frac{\partial f(p,t)}{\partial t} + v_{ax}\frac{\partial f(p,t)}{\partial ax} + eE(t)\frac{\partial f(p,\ t)}{\partial p_{ax}} = -\frac{[f(p,t) - f_0(p)]}{\tau} \tag{6}$$

where $f_0(p)$ is equilibrium Fermi distribution function, $f(p,t)$ is the distribution function, v_{ax} is the quasiparticle group velocity along the axis of CNT and τ is the relaxation time. The relaxation term of equation(6) describes the electron-phonon scattering, electron-electron collisions etc. Using the method originally developed in the theory of quantum semiconductor superlattice [16]. an exact solution of equation (6) can be constructed without assuming a weak electric field. Expanding the distribution functions of interest in Fourier series as [16, 23]

$$f(p,t) = \Delta p_\varphi \sum_{s=1}^{n} \delta(p_\varphi - s\Delta p_\varphi)\sum_{r\neq 0} f_{rs}e^{iarp_{ax}}\psi_v(t) \tag{7}$$

and

$$f_0(p) = \Delta p_\varphi \sum_{s=1}^{n} \delta(p_\varphi - s\Delta p_\varphi)\sum_{r\neq 0} f_{rs}e^{iarp_{ax}} \tag{8}$$

for zigzag CNTs.

where, $\delta(p_\varphi - s\Delta p_\varphi)$ is the Dirac delta function, f_{rs} is the coefficients of the Fourier series and $\psi_v(t)$ is the factor by which the Fourier transform of the nonequilibrium distribution function differs from its equilibrium distribution counterpart. We now determine the electric current density of the zigzag CNT.

By substituting equations (7) and (8) into equation (6), the below expression is obtained

$$\frac{\partial\psi_v(t)}{\partial t} + \left(iearE_{ax} + \frac{1}{\tau}\right)\psi_v(t) = \frac{1}{\tau} \tag{9}$$

Solving the homogeneous differential equation corresponding to equation (9), $\psi_v(t)$ is obtained as

$$\psi_v(t) = \frac{\hbar}{(\hbar + iraeE_{ax}\tau)} \tag{10}$$

The expression for the coefficients f_{rs} of equations (7) and (8) is found to be

$$f_{rs} = \frac{a}{2\pi\Delta p_\varphi}\int_0^{2\pi/a} \frac{\exp^{-iarp_{ax}}}{1 + \exp\{\varepsilon_s(p_{ax})/k_BT)\}}dp_{ax} \tag{11}$$

The surface current density is defined by

$$\begin{aligned} j_{ax} &= \frac{2e}{(2\pi\hbar)^2}\iint f(p,\ t)v_{ax}(p)d^2p \\ or \\ j_{ax} &= \frac{2e}{(2\pi\hbar)^2}\sum_{s=1}^{n}\int_0^{\frac{2\pi}{a}} f(p_{ax}, s\Delta p_\varphi, \psi_v(t))v_{ax}(p_{ax},\ s\Delta p_\varphi)dp_{ax} \end{aligned} \tag{12}$$

where the integration is over the first Brillouin zone, v_{ax} is given by

$$v_{ax}(p_{ax}, s\Delta p_\varphi) = \frac{\partial\varepsilon_s(p_{ax})}{\partial P_{ax}} \tag{13}$$

Now we expand $\varepsilon_s(p_{ax})/\gamma_0$ in Fourier series with coefficients ε_{rs} to be determined

$$\varepsilon(p_{ax}, s\Delta p_\varphi) = \varepsilon_s(p_{ax}) = \gamma_0\sum_{r\neq 0}\varepsilon_{rs}\exp^{iarp_{ax}} \tag{14}$$

The expression for the coefficients is found to be

$$\varepsilon_{rs} = \frac{a}{2\pi\gamma_0}\int_0^{2\pi/a} \varepsilon_s(p_{ax})\exp^{-iarp_{ax}}dp_{ax} \tag{15}$$

where $\varepsilon_s(p_{ax})$ is given by equation (3), from equations (13) and (14)

$$v_{ax}(p_{ax}, s\Delta p_\varphi) = \gamma_0\sum_{r\neq 0}\frac{\partial(\varepsilon_{rs}\exp^{iarp_{ax}})}{\partial p_{ax}} = \gamma_0\sum_{r\neq 0} iar\varepsilon_{rs}\exp^{iarp_{ax}} \tag{16}$$

From equation (7),

$$f(p_{ax}, s\Delta p_\varphi, \psi_v(t)) = \Delta p_\varphi\sum_{r\neq 0} f_{rs}\exp^{iarp_{ax}}\psi_v(t) \tag{17}$$

Substituting equations (5), (7) and (8) into equation (12) and considering only the real part of the current density j_{ax} for zigzag (n, 0) CNT we obtained

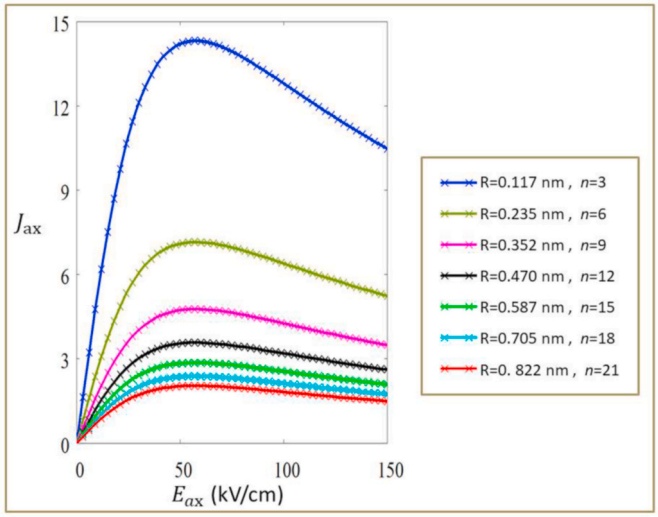

Fig. 1. A plot of normalized current density (J_{ax}) versus electric field (E_{ax}) for metallic zigzag (n, 0) CNTs where n = 3, 6, 9, 12, 15, 18 and 21 with the corresponding radius R = 0.117 nm, 0.235 nm, 0.352 nm, 0.470 nm, 0.587 nm, 0.705 nm and 0.822 nm respectively at T = 287.5 K.

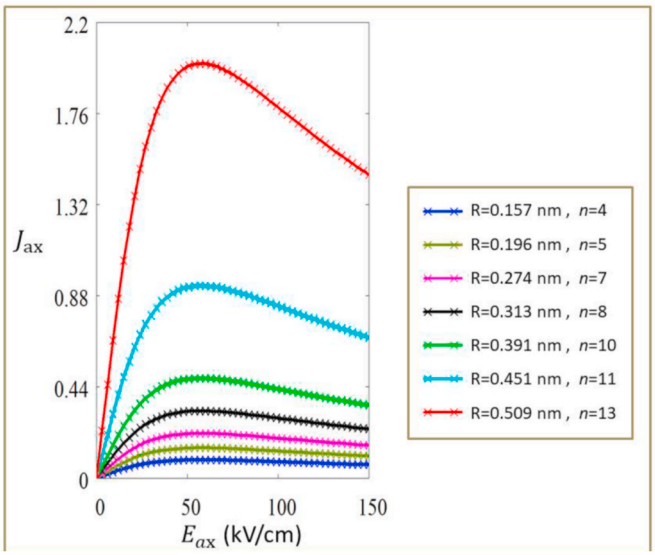

Fig. 2. A plot of normalized current density (J_{ax}) versus electric field (E_{ax}) for semiconducting zigzag (n, 0) CNTs where n = 4, 5, 7, 8, 10, 11 and 13 with the corresponding radius R = 0.157 nm, 0.196 nm, 0.274 nm, 0.313 nm, 0.391 nm, 0.431 nm and 0.509 nm respectively at T = 287.5 K.

$$j_{ax} = \frac{j_0}{n}\sum_{s=1}^{n}\left(\frac{a^2 n}{2\pi^2\sqrt{3}}\int_0^{2\pi/a}\frac{\exp^{-iarp_{ax}}}{1+\exp\left\{\left(\gamma_0\left[1+4cos(ap_{ax})cos\left(\frac{s\pi a}{n}\right)+4cos^2\left(\frac{s\pi a}{n}\right)\right]^{1/2}\right)\Big/k_BT\right)\right\}}dp_{ax}\right)\mathrm{x}$$
$$\left(\frac{a}{2\pi\gamma_0}\int_0^{2\pi/a}\left(\pm\gamma_0\left[1+4cos(ap_{ax})cos\left(\frac{s\pi a}{n}\right)+4cos^2\left(\frac{s\pi a}{n}\right)\right]^{1/2}\right)\exp^{-iarp_{ax}}dp_{ax}\right)\mathrm{x} \quad (18)$$
$$\sum_{r=1}^{\infty}\left(\frac{r^2 aeE_{ax}\tau\hbar}{\hbar^2+(raeE_{ax}\tau)^2}\right)$$

where $j_0 = \frac{4\sqrt{3}\,e^2\gamma_0}{\hbar^2}$ and n is the number of the unit vectors of hexagonal lattice of graphite sheet rolled up.

seamlessly to form the zigzag (n, 0) CNT. Also, the radius R of any type of CNTs is derived as $\mathrm{R} = \frac{\sqrt{3}a_{c-c}}{2\pi}(m^2+mn+n^2)^{\frac{1}{2}}$ [6] where a_{c-c} is the distance between adjacent carbon atoms in the flat sheet or the C–C bond length. For zigzag (n, 0) CNT, radius R is expressed in terms of number n of unit vector as

$$\mathrm{R} = \frac{\sqrt{3}a_{c-c}}{2\pi}n \text{ since } m = 0 \text{ for zigzag } (n,0)\text{CNTs and hence } n \text{ in terms}$$
$$\mathrm{R} \text{ is obtained as } n = 2\pi\mathrm{R}\Big/\sqrt{3}a_{c-c} \quad (19)$$

Substituting equations (4) and (19) into equation (18), we obtained the current density along the axis J_{ax} as function of dc field along the axis E_{ax} and radius R for zigzag (n, 0) CNT as

$$j_{ax} = \frac{\sqrt{3}\,a\hbar j_0}{3\pi\mathrm{R}}\sum_{s=1}^{n}\left(\frac{a\mathrm{R}}{2\sqrt{3}\pi\hbar}\int_0^{2\pi/a}\frac{\exp^{-iarp_{ax}}}{1+\exp\left\{\left(\gamma_0\left[1+4cos(ap_{ax})cos\left(\frac{\sqrt{3}sa^2\hbar}{3\mathrm{R}}\right)+4cos^2\left(\frac{\sqrt{3}sa^2\hbar}{3\mathrm{R}}\right)\right]^{1/2}\right)\Big/k_BT\right)\right\}}dp_{ax}\right)\mathrm{x}$$
$$\left(\frac{a}{2\pi\gamma_0}\int_0^{2\pi/a}\left(\gamma_0\left[1+4cos(ap_{ax})cos\left(\frac{\sqrt{3}sa^2\hbar}{3\mathrm{R}}\right)+4cos^2\left(\frac{\sqrt{3}sa^2\hbar}{3\mathrm{R}}\right)\right]^{1/2}\right)\exp^{-iarp_{ax}}dp_{ax}\right)\mathrm{x} \quad (20)$$
$$\sum_{r=1}^{\infty}\left(\frac{r^2 aeE_{ax}\tau\hbar}{\hbar^2+(raeE_{ax}\tau)^2}\right)$$

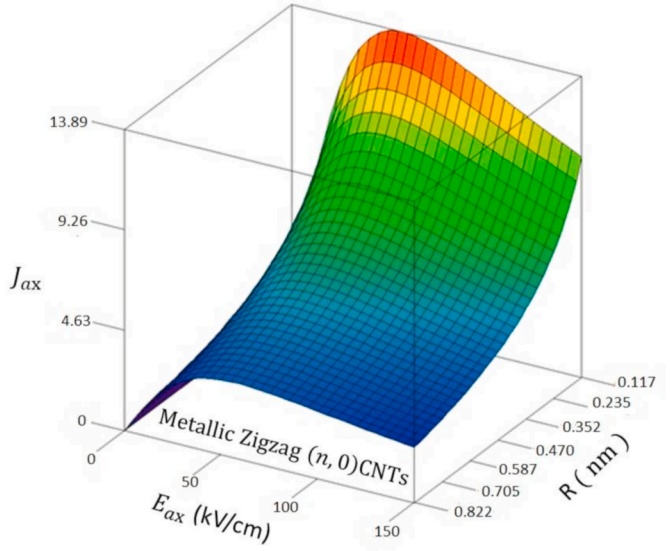

Fig. 3. 3D plot of normalized current density (J_{ax}) versus dc field (E_{ax}) and radius (R) for metallic zigzag (3, 0), (6, 0), (9, 0), (12, 0), (15, 0), (18, 0) and (21, 0) CNTs with the corresponding radius of 0.117 nm, 0.235 nm, 0.352 nm, 0.470 nm, 0.587 nm, 0.705 nm and 0.822 nm respectively at $T = 287.5$ K.

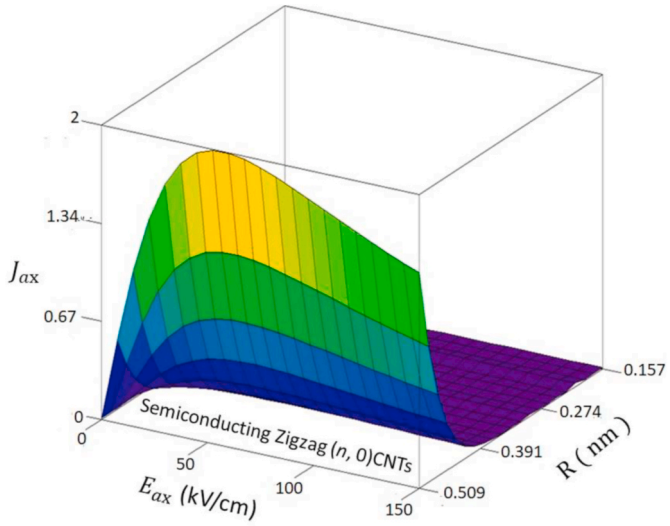

Fig. 4. 3D plot of normalized current density (J_{ax}) versus dc field (E_{ax}) and radius (R) for semiconducting zigzag (4, 0), (7, 0), (10, 0) and (13, 0) CNTs with the corresponding radius of 0.157 nm, 0.274 nm, 0.391 nm and 0.509 nm respectively at $T = 287.5$ K.

3. Results and discussions

The behaviour of normalized current density along the axis of the carbon nanotube ($J_{ax} = j_{ax}/j_0$) as a function of the applied dc field along the axis (E_{ax}) as the radius R of metallic zigzag (n, 0) CNT increases from 0.117 nm to 0.822 nm is displayed in Fig. 1. The radius dependence of the electrical conductivity of metallic zigzag (n, 0) CNTs is shown in the figure.

We have observed in Fig. 1 that the peak normalized current density and the electrical conductivity $\left|\frac{\partial J_{ax}}{\partial E_{ax}}\right|$ at any dc field (E_{ax}) represented by the tangent to the curve at that particular dc field (E_{ax}) for either ohmic region $\left(\text{i.e.}\frac{\partial J_{ax}}{\partial E_{ax}} > 0\right)$ or negative differential conductivity (NDC) region $\left(\text{i.e.}\frac{\partial J_{ax}}{\partial E_{ax}} < 0\right)$ decreases as the radius R of the metallic zigzag (n,0) CNT increases from 0.117 nm to 0.235 nm with the corresponding chiral index n of 3 and 6 respectively at a constant temperature of 287.5 K. As the radius R further increases from 0.235 nm and finally to 0.822 nm with the corresponding chiral index n of 6 and 21 respectively, the peak normalized current density and the electrical conductivity decrease further as shown in Fig. 1. This behaviour could be attributed to the fact that as the radius R of the zigzag (n, 0) CNT increases with a corresponding increase in chiral index n, the scattering rate of electrons also increases leading to the decrease in electrical conductivity as well as peak current density.

Also, the behaviour of normalized current density along the axis of the CNT ($J_{ax} = j_{ax}/j_0$) as a function of the applied dc field along the axis (E_{ax}) as the radius R of semiconducting zigzag (n, 0) CNT increases from 0.157 nm to 0.509 nm is displayed in Fig. 2. The radius dependence of the electrical conductivity of semiconducting zigzag (n, 0) CNTs is clearly shown in the Fig. 2.

From the Fig. 2, unlike metallic zigzag (n, 0) CNTs in Fig. 1, we have observed that the peak normalized current density and the electrical conductivity at any dc field (E_{ax}) for either ohmic or NDC region rather increase as the radius R of semiconducting zigzag (n, 0) CNT increases from 0.157 nm to 0.196 nm with the corresponding chiral index n of 4 and 5 respectively at a constant temperature of 287.5 K. As the radius R further increases from 0.196 nm and finally to 0.509 nm with the corresponding chiral index n of 5 and 13 respectively, the peak normalized current density and the electrical conductivity increase drastically as shown in Fig. 2. This could be attributed to the fact that n is directly proportional to the diameter D (or radius R) of the semiconducting zigzag (n, 0) CNTs. In semiconducting CNTs, D (or R) is inversely proportional to energy band gap [24–26]. Hence as the radius R (or diameter D) increases, the energy band gap of the semiconducting zigzag (n, 0) CNTs decreases accordingly resulting in more electrons in the valence band overcoming relatively narrow energy band gap into conduction band for conduction. This accounts for the increase in electrical conductivity as the radius R of semiconducting zigzag (n, 0) CNT increases.

To put the observed radius dependence of the electrical conductivity of zigzag CNTs in perspective, the 3-dimensional behaviour of the normalized current density (J_{ax}) as a function of the dc field (E_{ax}) and the radius (R) for metallic and semiconducting zigzag (n, 0) CNTs are displayed in Figs. 3 and 4 respectively.

In Fig. 3, the electrical conductivity and peak normalized current density of metallic zigzag (n, 0) CNT decrease with increasing radius from 0.117 nm to 0.822 nm with the corresponding chiral index n of 3 and 21 respectively. For metallic zigzag (n, 0) CNT, the electrical conductivity and the peak normalized current density are at the highest values when the radius of the tube is the lowest (i.e. R = 0.117 nm with the corresponding chiral index $n = 3$). As the radius gradually increases, the electrical conductivity and the peak normalized current density decrease until the lowest values are obtained at highest radius of 0.822 nm with the corresponding chiral index n of 21 as shown in Fig. 3.

Also in Fig. 4, the electrical conductivity and the peak normalized current density of semiconducting zigzag (n, 0) CNT increase with increasing radius from 0.157 nm to 0.509 nm with the corresponding chiral index n of 4 and 13 respectively. Unlike metallic zigzag carbon nanotube, the electrical conductivity and the peak normalized current density of semiconducting zigzag (n, 0) CNT are at the lowest values when the radius is the lowest (i.e. R = 0.157 nm with the corresponding chiral index $n = 4$). As the radius gradually increases, the electrical conductivity and the peak current density increase until the highest values are obtained at highest radius of 0.509 nm with the corresponding chiral index n of 13 as shown in Fig. 4.

Therefore, this study predicts metallic zigzag (3, 0) CNT with the least radius of 0.117 nm to be best conductor of electricity among all metallic zigzag (n, 0) CNTs. Furthermore, the study has shown that the electrical conductivity of semiconducting zigzag (n, 0) CNTs could be increased by just increasing the radius of that particular semiconducting zigzag (n, 0) CNTs without doping.

4. Conclusions

In conclusion, radius dependence of the electrical conductivity of metallic and semiconducting zigzag CNTs is theoretically studied using semiclassical approach. The theoretical framework investigation shows that the thinner metallic zigzag CNT and thicker semiconducting zigzag CNT are better conductors of electricity. This research therefore offers way of obtaining higher electrical conductivity in both materials without doping. This study therefore shows applications in the development of current conducting nano-devices for scientific systems.

Declaration of competing interest

No conflict of interest exists.

References

[1] Ahmad Aqel, Kholoud M.M. Abou El-Nour, Reda A.A. Ammar, Abdulrahman Al-Warthan, Carbon nanotubes, science and technology part (I) structure, synthesis and characterisation, Arab. J. Chem. 5 (1) (2012) 1–23.
[2] Bohua Sun, Formulation of 2D graphene deformation based on chiral-tube base vectors, J. Nanomater. (2010) 2010.
[3] E.N. Ganesh, Single walled and multi walled carbon nanotube structure, synthesis and applications, Int. J. Innovative Technol. Explor. Eng. 2 (4) (2013) 311–320.
[4] Mahdi Pourfath, Siegfried Selberherr, Current transport in carbon nanotube transistors, in: 2008 7th International Caribbean Conference on Devices, Circuits and Systems, IEEE, 2008, pp. 1–6.
[5] Jeroen WG. Wilder, Liesbeth C. Venema, Andrew G. Rinzler, Richard E. Smalley, Cees Dekker, Electronic structure of atomically resolved carbon nanotubes, Nature 391 (1998) 59–62, 6662.
[6] Jean-Christophe Charlier, Xavier Blase, Stephan Roche, Electronic and transport properties of nanotubes, Rev. Mod. Phys. 79 (2) (2007) 677.
[7] Chang Kook Hong, Hyun Seok Ko, Eun Mi Han, Kyung Hee Park, Electrochemical properties of electrodeposited PEDOT counter electrode for dye-sensitized solar cells, Int. J. Electrochem. Sci. 10 (7) (2015) 5521–5529.
[8] Valerie Jamieson, Carbon nanotubes roll on, Phys. World 13 (6) (2000) 29.
[9] G. Dresselhaus, Mildred S. Dresselhaus, Riichiro Saito, Physical Properties of Carbon Nanotubes, World scientific, 1998.
[10] Pulickel M. Ajayan, Otto Z. Zhou, Applications of carbon nanotubes, in: Carbon Nanotubes, Springer, Berlin, Heidelberg, 2001, pp. 391–425.
[11] Jan M. Schnorr, Timothy M. Swager, Emerging applications of carbon nanotubes, Chem. Mater. 23 (3) (2011) 646–657.
[12] Morinobu Endo, Michael S. Strano, Pulickel M. Ajayan, Potential applications of carbon nanotubes, in: Carbon Nanotubes, Springer, Berlin, Heidelberg, 2007, pp. 13–62.
[13] Mauricio Terrones, Science and technology of the twenty-first century: synthesis, properties, and applications of carbon nanotubes, Annu. Rev. Mater. Res. 33 (1) (2003) 419–501.
[14] Melissa Paradise, Tarun Goswami, Carbon nanotubes–production and industrial applications, Mater. Des. 28 (5) (2007) 1477–1489.
[15] Hongjie Dai, Carbon nanotubes: opportunities and challenges, Surf. Sci. 500 (1–3) (2002) 218–241.
[16] Anton S. Maksimenko, Ya Slepyan Gregory, Negative differential conductivity in carbon nanotubes, Phys. Rev. Lett. 84 (2) (2000) 362.
[17] Sulemana S. Abukari, Samuel Y. Mensah, Kofi W. Adu, Natalia G. Mensah, Kwadwo A. Dompreh, Twum Anthony, Chales LY. Amuah, Matthew Amekpewu, Musah Rabiu, Domain Suppression in the Negative Differential Conductivity Region of Carbon Nanotubes by Applied AC Electric Field, 2012.
[18] Matthew Amekpewu, Sulemana S. Abukari, Kofi W. Adu, Samuel Y. Mensah, Natalia G. Mensah, Effect of hot electrons on the electrical conductivity of carbon nanotubes under the influence of applied dc field, Eur Phys. J. B 88 (2) (2015) 13.
[19] M. Amekpewu, S.Y. Mensah, R. Musah, N.G. Mensah, S.S. Abukari, K.A. Dompreh, Hot electrons injection in carbon nanotubes under the influence of quasi-static ac-field, Phys. E Low-dimens. Syst. Nanostruct. 81 (2016) 145–149.
[20] Pei Yang, He Meng, Xiancheng Ren, Kai Zhou, Effect of carbon nanotube on space charge suppression in PP/EPDM/CNT nanocomposites, J. Polym. Res. 27 (5) (2020) 1–11.
[21] D.A. Ryndyk, N.V. Demarina, J. Keller, E. Schomburg, Superlattice with hot electron injection: an approach to a Bloch oscillator, Phys. Rev. B 67 (3) (2003), 033305.
[22] Min-Fa Lin, Kenneth W-K. Shung, Magnetization of graphene tubules, Phys. Rev. B 52 (11) (1995) 8423.
[23] M. Amekpewu, S.Y. Mensah, R. Musah, N.G. Mensah, S.S. Abukari, K.A. Dompreh, High frequency conductivity of hot electrons in carbon nanotubes, Phys. B Condens. Matter 488 (2016) 83–87.
[24] A. Rakitin, C. Papadopoulos, J.M. Xu, Electronic properties of amorphous carbon nanotubes, Phys. Rev. B 61 (8) (2000) 5793.
[25] Yuki Matsuda, Jamil Tahir-Kheli, A. William, Goddard III, Definitive band gaps for single-wall carbon nanotubes, J. Phys. Chem. Lett. 1 (19) (2010) 2946–2950.
[26] Richard Martel, T. Schmidt, H.R. Shea, T. Hertel, Ph Avouris, Single-and multi-wall carbon nanotube field-effect transistors, Appl. Phys. Lett. 73 (17) (1998) 2447–2449.